

Explosion Replication Test of FCEV Hydrogen Tank

Park, B. and Kim, Y[†]

¹ Researchers, Department of Fire Safety Research, Korea Institute of Civil Engineering

[†]Corresponding Author e-mail: yangkyunkim@kict.re.kr TEL: +82-31-369-0559, FAX: +82-31-369-0555

ABSTRACT

Due to the increased interest in alternative energy sources, hydrogen device safety has become paramount. In this study, we induced the explosion of a hydrogen tank from a fuel cell electric vehicle (FCEV) by igniting a fire beneath it and disabling the built-in temperature pressure relief device. Three Type 4 tanks were injected gaseous hydrogen at pressures of 700, 350, and 10 bar, respectively. The incident pressure generated by the tank explosion was measured by pressure transducers positioned at various points around the tank. A protective barrier was installed to examine its effect on the resulting damage, and the reflected pressure was measured along the barrier. The internal pressure and external temperature of the tanks were measured in multiple locations. The 700- and 350-bar hydrogen tanks exploded approximately 10 and 16 min after burner ignition, respectively. The 10-bar hydrogen tank did not explode, but ruptured approximately 29 min after burner ignition. The explosions generated blast waves, fireballs, and fragments. The impact on the surrounding area was evaluated and we verified that the blast pressure, fireballs, and fragments were almost completely blocked by the protective barrier. The results of this study are expected to improve safety on an FCEV accident scene.

1. INTRODUCTION

Carbon emission reduction is high on the global agenda, and related policies have been proposed to address the dependency on carbon-producing energy sources [1]. To meet this goal, Korea aims to rapidly transition to a hydrogen-based society through the Hydrogen Economy Promotion and Hydrogen Safety Management Act (Ministry of Trade, Industry and Energy, 2021). Additionally, Battery electric vehicle (BEV) is still the focus for the automotive industry with FCEV as an interesting option for some cases. Korea is known to have world-class automotive technologies and is set to supply FCEVs domestically and internationally by significantly investing in green vehicle research and development. As of July 2021, approximately 15,000 FCEVs are in use in Korea, accounting for 1.57% of low-carbon vehicles (including hybrid and EVs). As part of its Hydrogen Economy Roadmap (Ministry of Trade, Industry and Energy, 2019), the hydrogen mobility project plans to supply 6.2 million FCEVs and 1,200 hydrogen charging stations by 2040 [2, 3]. However, FCEVs utilize high-pressure hydrogen gas (700 bar), which poses safety risks and requires safety devices such as a relief valve and a thermal pressure relief device (TPRD). Hydrogen gas has a flammability range of 4 to 75% and can be easily ignited by static electricity, leading to a jet flame with a temperature up to 2207 °C [4]. Many drivers, firefighters, and civilians are concerned about the safety of FCEVs due to their use of hydrogen gas, which is also used to manufacture hydrogen bombs. To move forward with these technologies, assuring the public of the safety of FCEVs is imperative. One measure to that end requires verifying the minimum safe distance from the vehicle in the event of a jet flame or tank rupture, enhancing the safety measures of FCEVs.

Research on hydrogen safety has been focused on areas where hydrogen energy is prominently applied, such as hydrogen charging stations [5, 6], hydrogen-powered homes (fuel cell rooms) [7, 8], and FCEVs [9]. The fuel cell (FC) of an FCEV transforms the chemical energy of stored hydrogen in a hydrogen tank into electrical energy to run the engine. Current studies have applied catastrophic scenarios to hydrogen tanks, including artificially creating a pool fire accident under the tank [10, 11], inducing a jet flame by manipulating the TPRD [12], or removing the TPRD to simulate device failure [13–17]. Some of the findings of these studies have been incorporated into safety-related technical standards for green vehicles, such as ISO 17268 [18], SAE J2600 [19], EU 406 [20], and GB T26779 [21].

For this experiment, a heptane burner was placed directly below a commercially available FCEV hydrogen tank to replicate a pool fire accident. The TPRD of the tank was removed to increase the

internal pressure and create a worst-case scenario. The resulting tank explosion accident was measured and analyzed to determine the range of human and structure damage caused by the peak overpressure generated in the explosion. Based on the experimental results, we propose a safe separation distance in case of an FCEV accident, helping to ensure a safer implementation of FCEVs.

2. EXPERIMENTAL

2.1 Experimental setup

To minimize concussive interference when measuring the incident pressure, the experiment was conducted in a wide space (Fig. 1(a)). The experiment consisted of three explosion tests using three FCEV hydrogen tanks pressurized to 700 bar (2.1 kg H₂), 350 bar (1.05 kg H₂), and 10 bar (0.003 kg H₂), respectively. The pressure of each hydrogen tank was raised by an external fire source. The TPRD was removed, and the resulting opening was sealed to amplify the pressure within the tank.

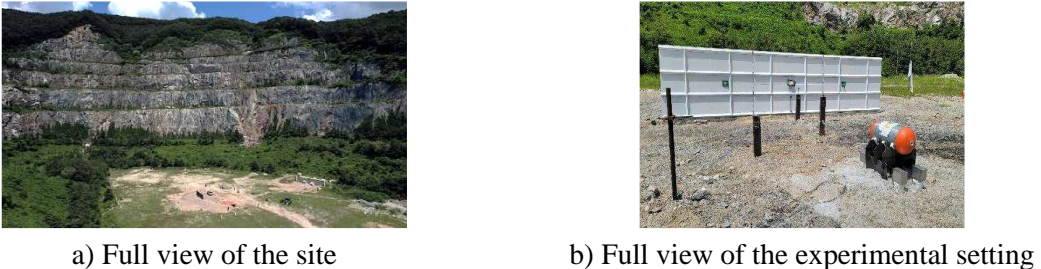


Figure 1. Experiment view

A FCEV hydrogen tank can compress and store hydrogen gas to a maximum pressure of 700 bar, which gradually drops as the electrical energy is consumed while driving, and the internal pressure of the hydrogen gas decreases. A TPRD is installed in each hydrogen tank of an HCEV. When the glass bulb of the TPRD reaches 110 °C or higher, indicating high internal pressure, it breaks and releases the hydrogen to lower the internal pressure [22]. The operation of the TRPD on one hydrogen tank allows the release of hydrogen gas only within the tank where the TPRD is installed. FCEVs use Type 4 tanks that have an inner polyamide liner coating and outer coating of carbon fiber over a plastic liner. Table 1 presents the specifications of a Type 4 FCEV hydrogen tank.

Table 1. Hydrogen tank model parameters.

Volume	Pressure	Gas Weight	Nozzle Size	Flow Rate	Length	Diameter
52.2 L	70 MPa	2.1 kg	1.8 mm	0.102 kg/s	870 mm	363 mm



(a) Heptane nozzles and ignitor (b) Heptane fuel tank and supply system (c) Installed protective barrier

Figure 2. Snapshots of the accident scenario replication devices

The explosion tests were conducted following the UN GTR 13 protocol [10, 11], replicating a pool fire accident under a hydrogen tank. As shown in Fig. 2(a), a heptane burner with twelve spray nozzles, designed to release heptane at a flow rate of 0.9 LPM, and a mounted ignitor were positioned beneath the tank. The arrangement of the pressure transducers relative to the hydrogen tank and a protective barrier is shown in Fig. 3. A 4.5-mm-thick steel (2 m × 10 m) protective barrier was installed on a reinforced concrete base, following the steel panel protective barrier installation standard (KGS FP217 [24]). Three reflected pressure transducers (1.2 meters high) were positioned over the protective barrier, as shown in Fig. 4(c).

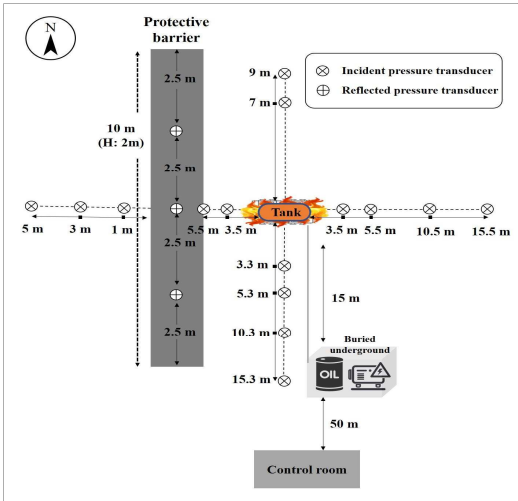


Figure 3. Arrangement of measurement devices

When measuring the peak overpressure, two separate components were measured: incident and reflected overpressures. Fifteen incident pressure transducers (H:1.5m) were positioned along the four cardinal directions, with the hydrogen tank placed at the center of the arrangement. Four units were placed to the east of the tank (at distances of 3.5, 5.5, 10.5, and 15.5 m), two units to the west (3.5 and 5.5 m), four units to the south (3, 5, 10, and 15 m), and two units to the north (7 and 9 m). The protective barrier was installed 5 m to the west of the tank, and three incident pressure transducers were positioned behind the barrier (at distances of 1, 3, and 5 m from the barrier). The fuel tank and supply system were installed underground 15 m from the hydrogen tank. The experiment was conducted from a control room located 50 m from the explosion test site. Specifications of the measurement devices are listed in Table 2. A data logger was used to record the electric signals transmitted from the fifteen incident pressure transducers and three reflected pressure transducers (Fig. 4) at a data transmission rate of 1 million samples per second.






a) Incident pressure transducer (blast pressure pencil probe, PCB)



b) Reflected pressure transducer

Figure 4. Photos of the measurement devices

Table 2. Specification of the measurement devices.

Measurement Devices		Specifications	Photos
Data logger	Operational temperature range	-20 ~ 50 °C	
	Measurement speed	≤ 1 MS/s	
	Number of channels	16 ch × 2 set	
	Measurement capabilities	strain gauge, strain gauge transducer, thermocouple, platinum RTD, DC voltage	
Incident pressure transducer	Pressure range	3.45 ~ 17.24 bar	
	Temperature range	-73 ~ 135 °C	
	Frequency range	≥ 400 kHz	
	Measurement item	Side-on overpressure	
Reflected pressure transducer	Maximum pressure	17.24 bar	
	Temperature range	-73 ~ 135 °C	
	Frequency range	500 kHz	
	Measurement items	Reflected overpressure and side-on overpressure	

As illustrated in Fig. 5, five thermocouples (K-Type) were placed around the tank: one each on the left, right, and top and two on the underside of the tank. The data transmission rate was set to five samples per second.

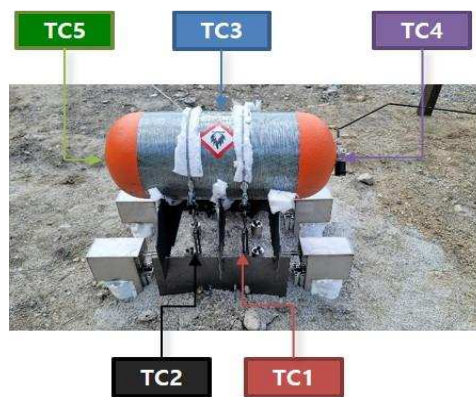


Figure 5. Thermocouple measurement locations

2.2 Progress of the explosion tests

The fire, which was ignited at the bottom of the hydrogen tank, gradually spread and eventually engulfed the entire tank. The 700-bar hydrogen tank exploded 10 min, 22 s after burner ignition; the 350-bar hydrogen tank exploded after 16 min, 13 s. The 10-bar hydrogen tank did not explode, but its internal pressure rose to 20 bar before the tank ruptured, approximately 29 min after burner ignition. The remaining hydrogen gas inside the tank escaped over the following 10 min until no hydrogen gas remained. The explosions were accompanied by blast waves, fireballs, debris, fragments, and mushroom

clouds. Following the explosion, the heptane supply to the burner was disabled, although the fire continued for some time before being extinguished by a standby fire truck (Fig. 6).

During the 700-bar hydrogen tank, the east side of the tank ruptured sending the tank west, where it collided with the barrier and then landed 7 m to the south. The 350-bar hydrogen tank ruptured in the middle and then landed 5 m to the south.

Pre-explosion		
		
(a) View from Head-on	(b) View from behind protective barrier	(c) View from in front of protective barrier
700-bar hydrogen tank		
		
(d) Mid-explosion	(e) Post-explosion (tank holder and ignitor)	(f) Post-explosion (debris)
350-bar hydrogen tank		
		
(g) Mid-explosion	(h) Post-explosion (tank holder and ignitor)	(i) Post-explosion (debris)
10-bar hydrogen tank		
		
		(j) Post-rupture

Figure 6. Views of the test apparatus (a)–(c) before the explosion, (d)–(f) during and after the 700-bar hydrogen tank explosion, (g)–(i) during and after the 350-bar hydrogen tank explosion, and (j) after the 10-bar hydrogen tank rupture

2.3 Characterization of the materials

The maximum recorded pressures at each pressure transducer location are shown in Fig. 7. Notably, the three transducers failed to record data during the 350-bar hydrogen tank explosion test.

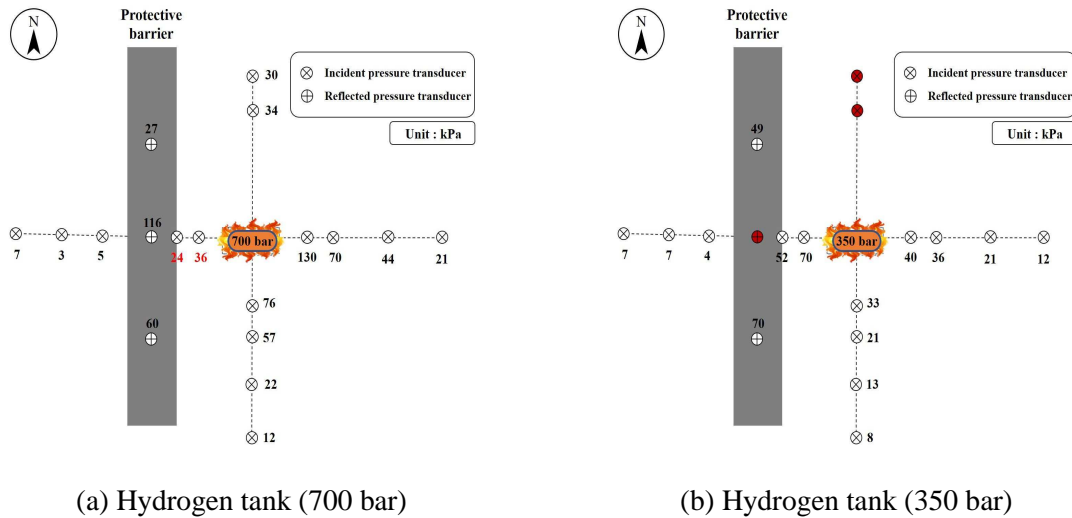


Figure 7. Values measured by the transducers at their respective positions

The 700-bar hydrogen tank exploded 10 min, 22 s after burner ignition. Within 0.08 s of the explosion, the peak incident and reflected overpressures were measured at 3–130 kPa and 27–116 kPa, respectively, as shown in Fig. 8. The maximum peak incident overpressure (130 kPa) was measured at 3.5 m east of the tank, and the second highest (76 kPa) at 3.3 m south of the tank. After passing the protective barrier, the peak overpressure weakened to one-tenth of its initial level, measuring at 3–7 kPa. Peak overpressure values measured by the transducers placed south of the tank were approximately half the level of those measured by the transducers placed east of the tank. Peak overpressure values measured by the transducers placed west of the tank were very low, 24–36 kPa, owing to the impact of debris generated at the time of the explosion. As shown in Fig. 8, the reflected overpressure at the center of the protective barrier was two and four times higher than that measured by the transducers placed to the south and north, respectively.

The 350-bar hydrogen tank exploded 16 min, 13 s after burner ignition. Within 0.08 s of the explosion, the peak incident and reflected overpressures were measured at 4–70 kPa and 49–70 kPa, respectively, as shown in Fig. 9. No measurements were recorded by the north-side incident or reflected pressure transducer at the center of the protective barrier. The maximum peak incident overpressure (70 kPa) was measured at 3.5 m west of the tank, and the second highest (40 kPa) at 3.5 m east of the tank. After passing the protective barrier, the peak overpressure weakened to one-tenth of its initial level, measuring a reflected overpressure of 4–7 kPa. Peak incident overpressure values measured by the south-side transducers were approximately half the level of those measured by the west-side transducers, while those measured by the east-side transducers were three-fourth the level of those measured on the south-side.

For each test, the resulting impulse was calculated by integrating the positive values of the incident overpressure value (overpressure–time graph). The impulse at 0.08 s after each explosion was calculated, as shown in Figs. 8 and 9. The impulse is used, along with the maximum peak incident overpressure, to predict the level of human and property damage. In general, the values of the impulse and maximum peak incident overpressure are positively correlated. The impulse was measured as lower than the maximum peak incident overpressure at 3.5 m to the west of the 700- and 350-bar hydrogen tanks presumably due to the influence of debris and fragments from the ruptured hydrogen tank. Figure

10 highlights the incident overpressure and impulse from each explosion as a function of distance from the tank.

According to the experiment performed with the 700-bar hydrogen tank, the highest impulse of 212.20 Pa·s was measured at 3.5 m to the east, and the second highest impulse of 136.97 Pa·s was measured at 5.5 m to the east. In the case of the 350-bar hydrogen tank, the two highest impulse values were 159.28 Pa·s at 5.5 m to the west and 105.16 Pa·s at 3.3 m to the south.

The maximum peak incident overpressure and impulse measured in the 700-bar hydrogen tank during the explosion were 60 kPa and 52.92 Pa·s, which were 1.8 and 1.3 times higher, respectively, compared to those measured in the 350-bar hydrogen tank.

The reflected overpressures, as measured at the protective barrier, are demonstrated in Fig. 11.

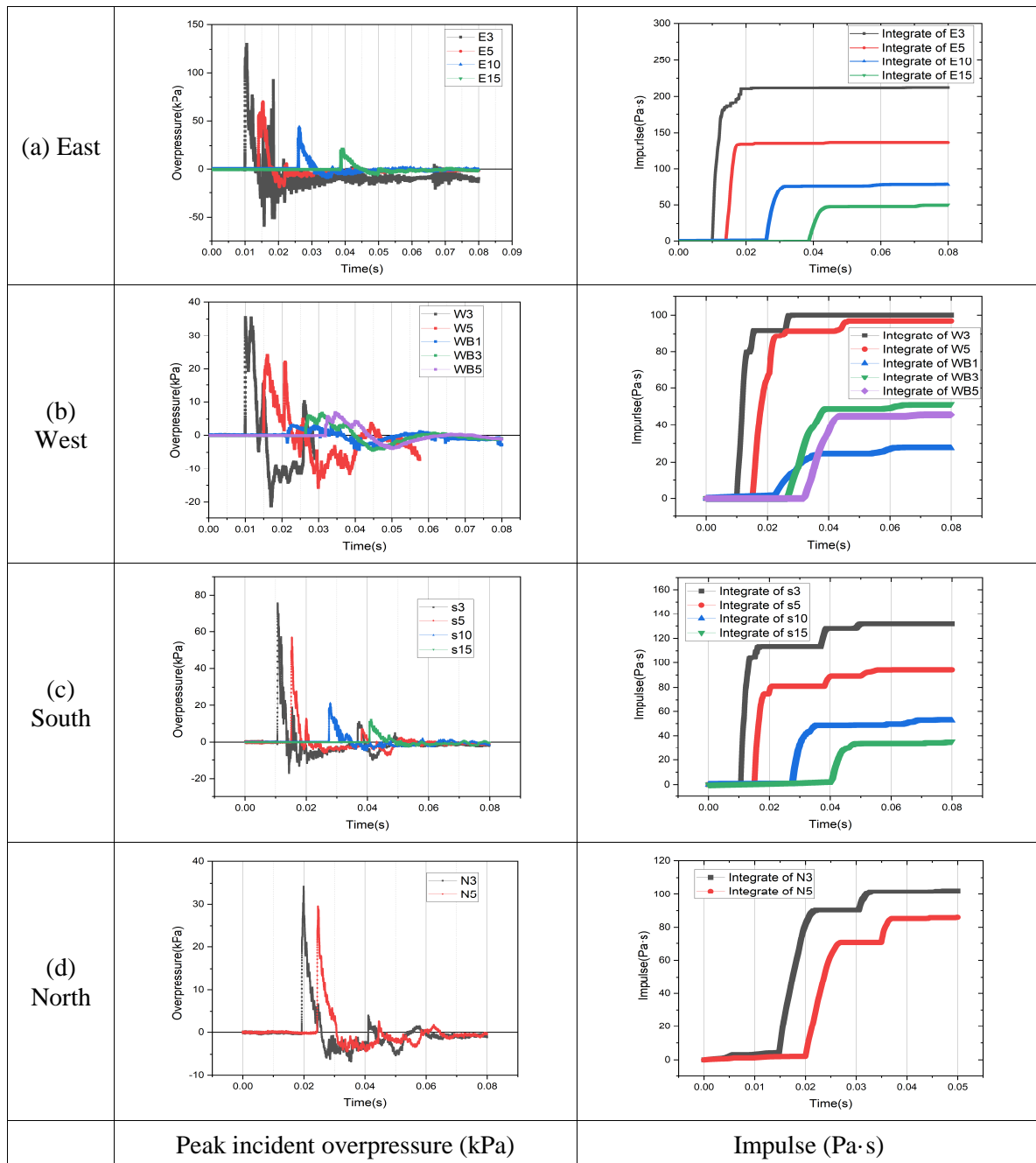


Figure 8. Peak incident pressure and impulse graphs (700 bar)

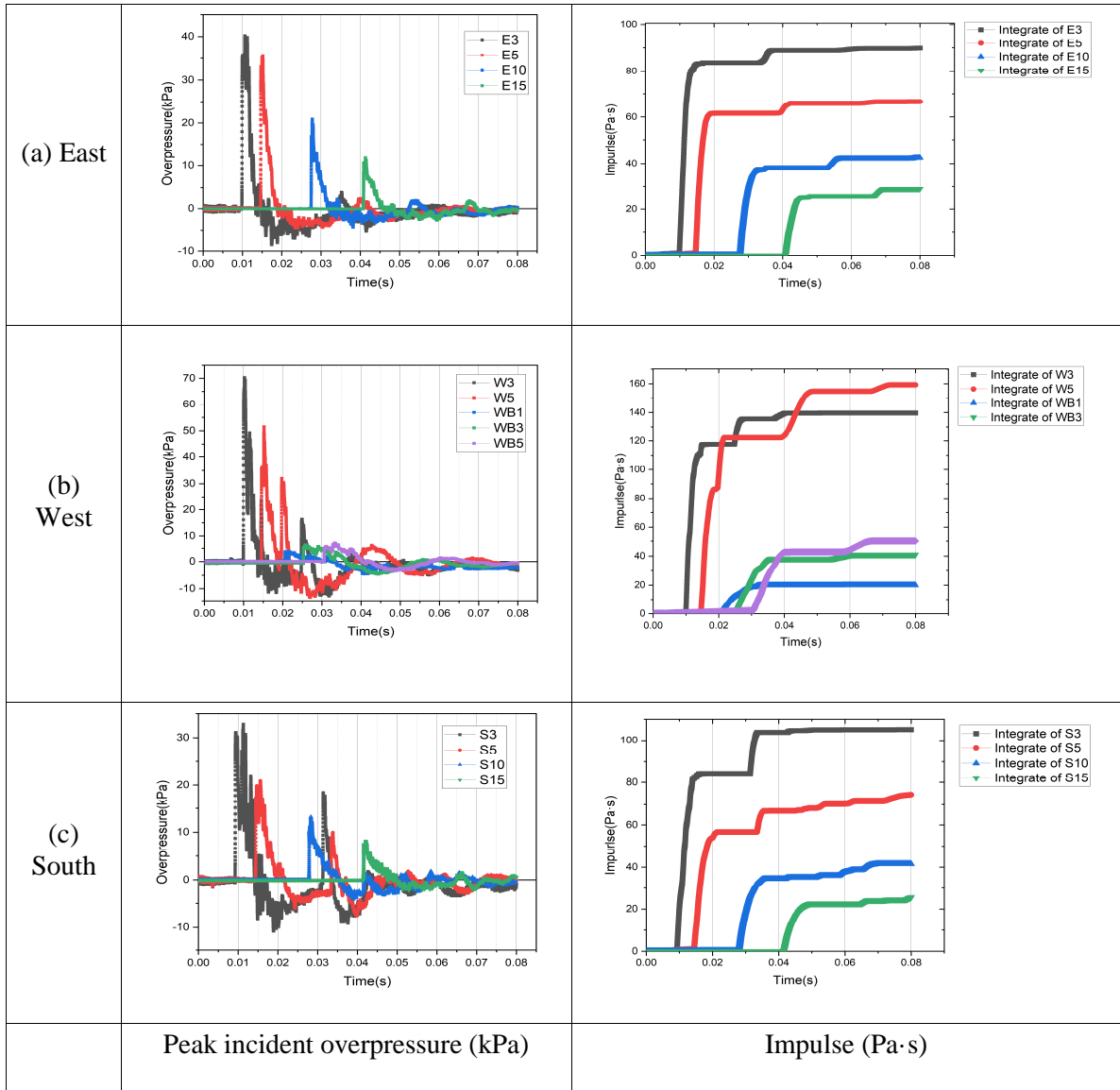


Figure 9. Peak incident overpressure and impulse graphs (350 bar)

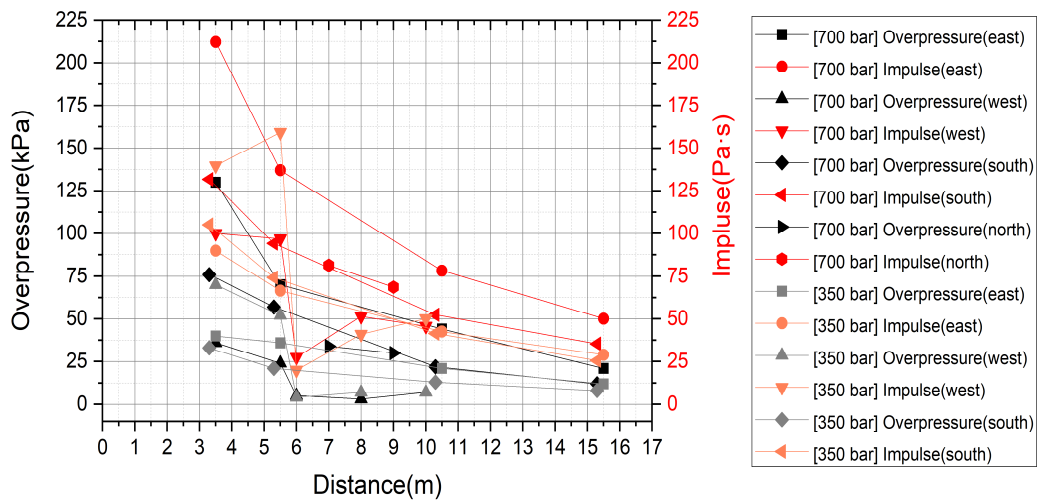
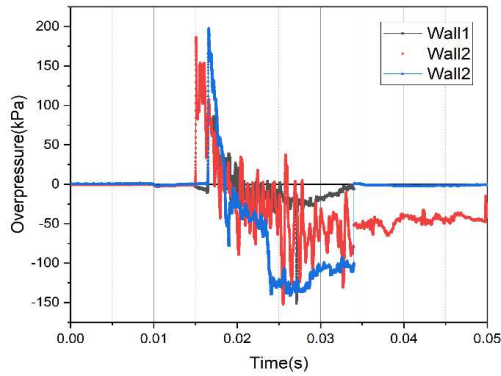
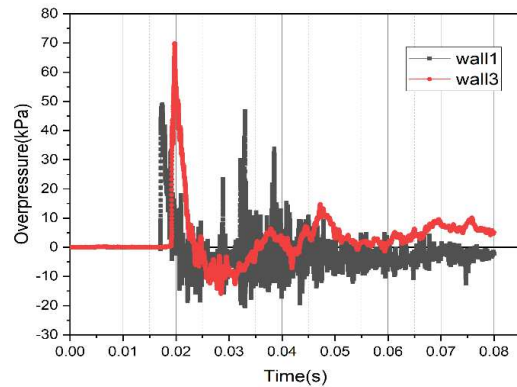


Figure 10. Peak incident and reflected overpressure and impulse as a function of distance from the tank



(a) Hydrogen tank (700 bar)



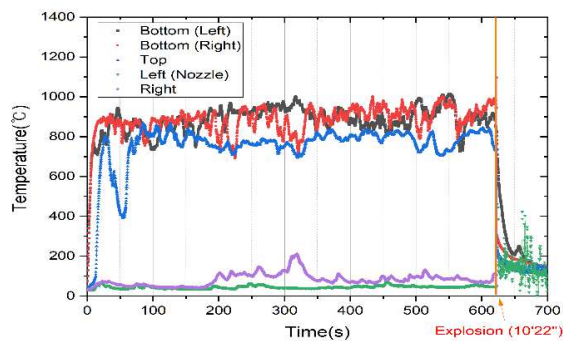
(b) Hydrogen tank (350 bar)

Figure 11. Reflected overpressure graphs as a function of time

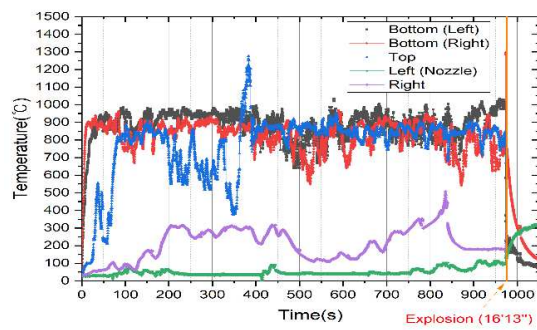
Changes in the tank temperatures over time are plotted in Fig. 12. Two thermocouples, installed on the underside of the 700-bar hydrogen tank, measured similar temperatures to each other, but consistently reported temperatures 100-200 °C higher than those reported by the thermocouple installed on the top. A thermocouple on the right (east) side of the tank consistently measured temperatures 50–100 °C higher than that on the left (west). After the heptane burner was lit for 200 s, the tank itself started to burn, and the fire spread across the tank. The temperature was measured at approximately 800–1000 °C at the bottom and top of the hydrogen tank.

The temperatures measured for the 350-bar and 700-bar hydrogen tanks test were similar. The temperatures measured at the top and the underside of the tank were also similar. However, at the top of each tank, the temperature dropped to 350 °C between 200-300 s after burner ignition and then rapidly increased to 1300 °C within the next 50 s. The right (east) side of the 350-bar hydrogen tank was approximately 100 °C higher than that in the 700-bar hydrogen tank in the same time period.

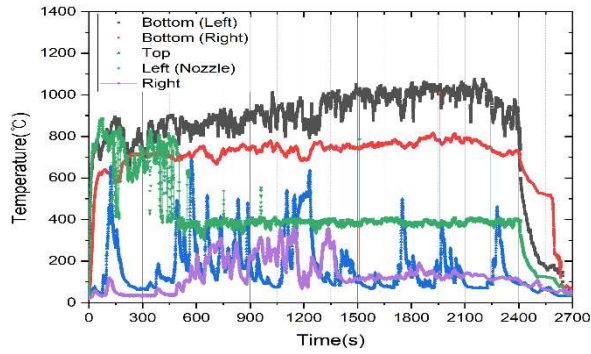
Changes in the internal pressure of each hydrogen tank are plotted as a function of time in Fig. 13. The data transmission rate was set to one sample every 0.25 s. The internal pressure of the 700-bar hydrogen tank increased to 760 bar in the time leading up to the explosion at 10 min, 22 s after burner ignition. The internal pressure of the 350-bar hydrogen tank increased to 446 bar in the time leading up to the explosion at 16 min, 13 s after burner ignition. The internal pressure of the 10-bar hydrogen tank increased to 20 bar approximately 29 min after burner ignition, after which the tank ruptured and the internal pressure rapidly dropped to 4 bar. Approximately 10 min were required for the remaining hydrogen gas to escape from the tank until the internal pressure finally fell to 0 bar, 40 min after burner ignition.



(a) Hydrogen tank (700 bar)

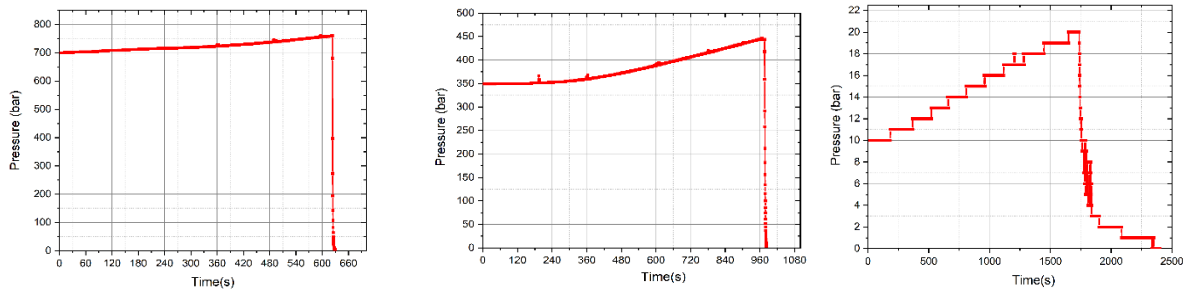


(b) Hydrogen tank (350 bar)



(c) Hydrogen tank (10 bar)

Figure 12. Temperature readings of the tank as a function of burn time



(a) Hydrogen tank (700 bar)

(b) Hydrogen tank (350 bar)

(c) Hydrogen tank (10 bar)

Figure 13. Internal pressure as a function of time

After each experiment, the protective barrier was examined for damage and tank fragments and debris were located, as shown in Fig. 14. The surface of the Type 4 model hydrogen tank is made of carbon fiber, which weakens when exposed to fire. During the 700-bar test, the east side of the barrier (facing the explosion) lost physical strength quickly due to the prevailing east wind and consequent debris scattering to the west. During the 350-bar test, light winds were observed, and the bottom center of the tank was the source of the primary rupture, causing debris to scatter to the south. During both explosions, blackened carbon fibers were scattered up to 10 m from the tank and the tank holder was bent. Fragments from the 700-bar test tank collided with the 4.5-mm-thick steel protective barrier, creating a 4 cm hole, and violently shook the concrete base, leaving cracks within it. The accumulated major debris of the 700-bar and 350-bar test tanks weighed 25.9 kg and 42.1 kg, respectively. Fragments weighing more than 4.5 kg, the typical weight of the head of a 70 kg man, can be lethal owing to the resulting concussion [24]. If the debris of the 700-bar hydrogen tank had scattered away from the barrier, the energy likely would have projected the is over 70 m from the initial location of the tank.

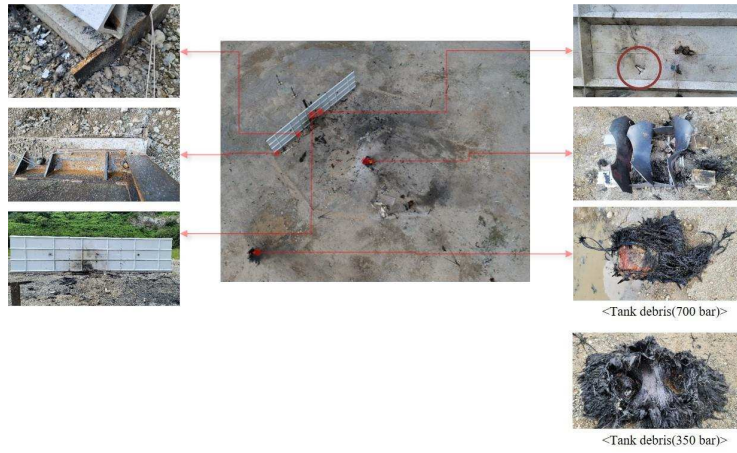
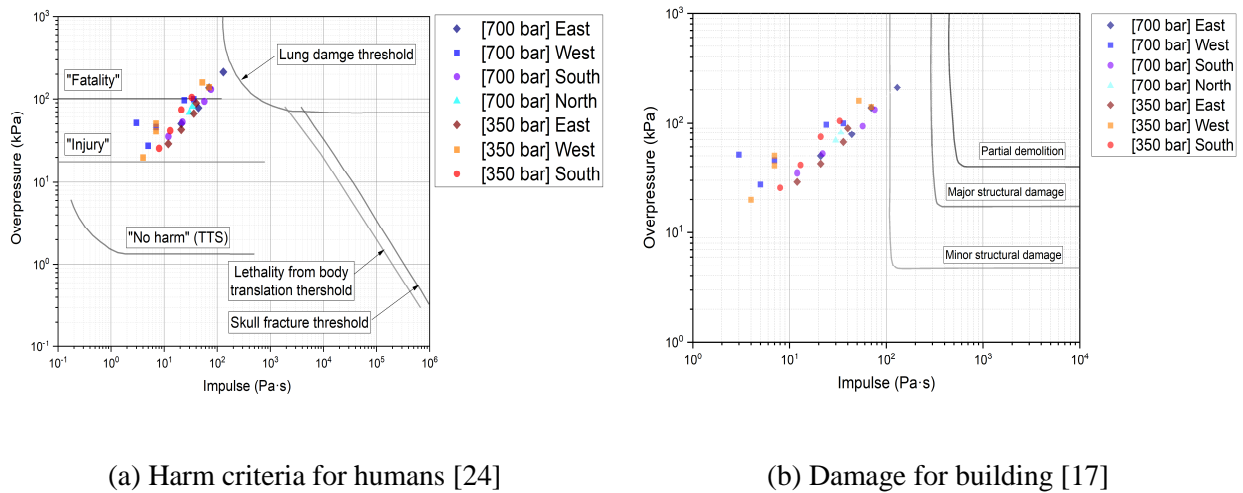


Figure 14. Distribution of fragments and debris

3. DISCUSSION

Fig. 15 plots the maximum peak overpressure and impulse values measured in this study relative to previously determined damage criteria for humans and buildings.



(a) Harm criteria for humans [24]

(b) Damage for building [17]

Figure 15. Overpressure-impulse thresholds

The human safety distance is the distance outside of which no temporary hearing loss occurs, called a temporary threshold shift (TTS) [25]. A blast wave with a magnitude of 16.5 kPa or higher can cause barotrauma of the human ear (eardrum rupture), and that of 100 kPa or higher results in life-threatening pulmonary hemorrhage [26, 24]. Based on the measured peak overpressures, there is a near certainty of eardrum rupture at 5 m from an explosion, and a high likelihood of fatality as far away as 3.5 m. Blast waves with an overpressure greater than 4 kPa and an impulse greater than 100 kPa can cause minor structural damage to buildings, such as shattered windows. Therefore, any building within approximately 5 m of a tank explosion will likely have minor damage.

4. CONCLUSIONS

Given the global priority to achieve carbon neutrality, various policies have been proposed to address the current dependency on carbon-producing energy sources. The Korean government has prioritized the use of hydrogen energy as part of its roadmap to achieve carbon neutrality. As a result, significant research has focused on developing methods to utilize hydrogen gas as an energy source, with a particular emphasis on hydrogen mobility and the safe storage of compressed hydrogen gas. To ensure

safe utilization of hydrogen energy, numerous safety devices and standards have been implemented. This study focused on a worst-case scenario in which the TPRD of a hydrogen tank fails during a pool fire at the bottom of a FCEV. We conducted these explosion tests to estimate the damage caused by the blast waves generated by the explosion. The test results can be summarized as follows:

1) When a pool fire was ignited by a heptane burner underneath a hydrogen tank with a disabled TPRD, the 700- and 350-bar hydrogen tanks exploded after 10 min, 22 s and 16 min, 13 s, respectively, resulting in blast waves, followed by fireballs and black mushroom clouds.

2) The incident overpressure and reflected overpressure were measured and the impulse was calculated at 0.08 s after the explosion. The maximum peak incident overpressure and impulse measured in the 350-bar test explosion were 33.3 kPa and 40.73 Pa·s, respectively. The maximum peak incident overpressure and impulse measured in the 700-bar test explosion were 60 kPa and 52.92 Pa·s, 1.8 and 1.3 times higher, respectively, than those of the 350-bar explosion. The protective barrier attenuated the incident overpressure to one-tenth of its initial level.

3) The internal pressure of the 700-bar and 350-bar hydrogen tanks rose to 760 bar and 446 bar, respectively, immediately before explosion. The 10-bar hydrogen tank did not explode, but ruptured at 20-bar after 29 minutes of burning.

4) During the 700-bar test, the fragmented debris violently collided with the 4.5-mm-thick steel protective barrier, creating a 4 cm hole in the barrier. Additionally, the carbon fiber lining of the tank scattered up to 10 m away from the tank.

Hydrogen gas tanks used in hydrogen mobility applications operate at higher pressures than general-purpose gas tanks, leading to different fire and explosion patterns. This necessitates a review of accident response manuals for hydrogen gas tank accidents, and the findings of this study can be integrated into standard operating procedures to improve safety. A follow-up study is planned to explore methods for safely managing and utilizing hydrogen energy for users, managers, and firefighters.

Competing Interests

There are no competing interests to declare.

Acknowledgements

Funding

This work was funded by a Fire Safety Agency's Energy Storage System Hydrogen Facility for Fire Safety, Technology, Research, and Development project [grant number 20008021].

References

- [1] Menon NV, Chan SH. Technoeconomic and environmental assessment of HyForce, a hydrogen-fuelled harbour tug. *Int J Hydrog Energy*. 2022;47:6924–35. <https://doi.org/10.1016/j.ijhydene.2021.12.064>.
- [2] Park S. Hydrogen economy revitalization road map, Korean Ministry of Trade, Industry and Energy, department of new energy industry, <https://www.iea.org/policies/6566-korea-hydrogen-economy-roadmap-2040>, http://www.motie.go.kr/motie/ne/presse/press2/bbs/bbsView.do?bbs_seq_n=161262&bbs_cd_n=81¤tPage=1&search_key_n=&cate_n=&dept_v=&search_val_v=; 2019.
- [3] Chu KH, Lim J, Mang JS, Hwang MH. Evaluation of strategic directions for supply and demand of green hydrogen in South Korea. *Int J Hydrog Energy*. 2022;47:1409–24. <https://doi.org/10.1016/j.ijhydene.2021.10.107>.
- [4] Crowl DA, Jo YD. The hazards and risks of hydrogen. *J Loss Prev Process Ind*. 2007;20:158–64. <https://doi.org/10.1016/j.jlp.2007.02.002>.
- [5] Park B, Kim Y, Paik S, Kang C. Numerical and experimental analysis of jet release and jet flame length for qualitative risk analysis at hydrogen refueling station. *Process Saf Environ Prot*. 2021;155:145–54. <https://doi.org/10.1016/j.psep.2021.09.016>.

- [6] Park B, Kim Y, Lee K, Paik S, Kang C. Risk assessment method combining independent protection layers (IPL) of layer of protection analysis (LOPA) and RISKCURVES software: Case study of hydrogen refueling stations in urban areas. *Energies*. 2021;14:4043. <https://doi.org/10.3390/en14134043>.
- [7] Park B, Kim Y, Hwang I. An experimental study on the explosion hazards in the fuel cell room of residential house. *J Kor Soc Saf*. 2021;36:71–9.
- [8] Park B, Kim Y. Experimental and analytical study on hydrogen-air deflagrations in open atmosphere. *J Kor Soc Saf*. 2021;36:64–71.
- [9] Choi Y, Jang G, Kim S, Hang K, Hang I, Ahn B et al. Fire safety evaluation of high pressure hydrogen system for FCEV. *Trans Korean Hydrog New Energy Soc*. 2009;20:188–93.
- [10] United Nations. Global technical Regulation No. 13—Global technical regulation on hydrogen and fuel cell vehicles. ECE/TRANS/180/Add.13; 2013.
- [11] Localized Fire test for improve reproducibility – Selection of standardized burner, GTR No. 13 TF #4; 2019.
- [12] Tamura Y, Takahasi M, Maeda Y, Mitsuishi H, Suzuki J, Watanabe S. Fire exposure burst test of 70-MPa automobile high-pressure hydrogen cylinders. In: *Proceedings of the Society of Automotive Engineers of Japan Annual Autumn Congress*, 28 September 2006, Sapporo, Japan.
- [13] Park JO, Yoo YH, Kim HW. An experimental study on the explosion of hydrogen Tank for fuel-cell electrical vehicle in semi-closed space. *J Auto-veh Saf Assoc*. 2021;13:73–80.
- [14] Zalosh R, Weyandt N. Hydrogen fuel tank Fire exposure burst test. *SAE Tech Pap*. 2005;114:2338–43. <https://doi.org/10.4271/2005-01-1886>.
- [15] Zalosh R. Blast waves and fireballs generated by hydrogen fuel tank rupture during fire exposure. In: *Proceedings of the 5th international seminar on fire and explosion hazards*. Edinburgh, UK: University of Edinburgh; 2007.
- [16] Molkov V, Kashkarov S. Blast wave from a high-pressure gas tank rupture in a fire: Stand-alone and under-vehicle hydrogen tanks. *Int J Hydrog Energy*. 2015;40:12581–603. <https://doi.org/10.1016/j.ijhydene.2015.07.001>.
- [17] Kashkarov S, Li Z, Molkov V. Blast wave from a hydrogen tank rupture in a fire in the open: Hazard distance nomograms. *Int J Hydrog Energy*. 2020;45:2429–46. <https://doi.org/10.1016/j.ijhydene.2019.11.084>.
- [18] International Organization for Standardization, ISO 17268. Gaseous hydrogen land vehicle refueling connection devices; 2020.
- [19] Society of Automotive Engineers. SAE J2600. Compressed hydrogen surface vehicle fueling connection devices; 2017.
- [20] Commission regulation, EU 406, implementing regulation (EC) No 79/2009 of the European Parliament and of the Council on Type-Approval of Hydrogen-Powered Motor Vehicles; 2010.
- [21] National standard of the People’s Republic of China, GB T26779. Hydrogen fuel cell electric vehicle refueling receptacle; 2021.
- [22] Hyundai Motors NEXO. Emergency response guide, <https://owners.hyundaiusa.com/content/dam/hyundai/us/myhyundai/manuals/erg/2019/nexo-fuel-cell/Nexo-Hydrogen-fc-erg.pdf>; 2019.
- [23] Korea Gas safety code, KGS FP216, code for facilities, technology and inspection for vehicle refueling by delivery of compressed hydrogen; 2019.
- [24] Debroey J. Probit function analysis of blast effects on human beings. Brussels, Belgium: Royal Military Academy; 2016.
- [25] Baker WE, Cox PA, Westine PS, Kulesz JJ, Strehlow RA. *Explosion hazards and evaluation*. Elsevier Scientific Publishing Company; 1983.
- [26] Center for Chemical Process Safety. Guidelines for evaluating the characteristics of vapour cloud explosions, flash fires, and BLEVEs. American Institute of Chemical Engineers; 1994, p. 347–57.